Defect-Induced Crystal-to-Amorphous Transition in an Atomistic Simulation Model

Horngming Hsieh and Sidney Yip
Department of Nuclear Engineering, Massachusetts Institute of Technology, Cambridge, Massachusetts 02139
(Received 12 August 1987)

Molecular-dynamics simulations of insertion of self-interstitials into a single fcc crystal reveal a crystal-to-amorphous transition which is dependent upon both insertion rate and defect-concentration accumulation. The resulting amorphous structure is found to be similar to that of a rapidly quenched liquid. In terms of elastic properties, amorphization brings about a further decrease in C_{11} and C_{44} relative to a defective crystal.

PACS numbers: 61.20.Ja, 61.40.+b, 61.80.Jh, 62.20.Dc

The phenomenon of amorphization of crystalline materials by electron- and ion-beam bombardment[1] is of fundamental interest from the standpoint of formation and stability of amorphous states of matter. It is also of considerable technological importance because of the potential of material modifications by irradiations.[2] Despite a rapidly growing body of experimental data, current understanding of the role of point defects in such questions as the nature of the driving force and the mechanism of the transformation is still incomplete. Since point-defect structures and interactions can be analyzed in great detail by molecular-dynamics simulation, it seems therefore useful to apply this technique to probe the crystal-to-amorphous transition under well characterized conditions.

In this Letter we report simulation results on the response of a monatomic crystalline lattice to the random insertions of self-interstitials. The study is part of an attempt[3] to model the phenomenon of radiation-induced amorphization through the introduction of Frenkel pairs or self-interstitials. Here we focus on the effects of the interstitials because they are believed to be dominant in destabilizing the lattice. In the following we will show that the amorphization threshold is dependent upon both defect concentration and insertion rate; furthermore, the defect-induced amorphous state is structurally very similar to a vitrified state obtained by quenching of a liquid.

The method of simulation we employ is fairly standard.[3] The equations of motion for a periodic system of particles interacting via the Lennard-Jones (6-12) potential with parameters σ and ϵ are integrated with use of a fifth-order predictor-corrector algorithm, and the vectors defining the simulation cell are allowed to change in response to any imbalance between the internal and the external stresses.[4] Prior to any defect insertion the system is an fcc lattice containing 576 atoms with the z axis oriented along [111]. Each self-interstitial is randomly introduced at the center of a cell formed by three nearest neighbors of a particle, a position which corresponds to the octahedral site in an fcc unit cell.[3] A time-step size of $\Delta t = 0.01$ is used; however, to allow for dissipation of local heating immediately following an insertion, the time step is decreased by a factor of 20 and gradually brought back to normal. All the results reported here are given in dimensionless units where length is scaled by σ, energy by ϵ, and time by τ, where $\tau = \sigma(m/\epsilon)^{1/2}$ and m is the particle mass.

The simulation consists of two stages, an "irradiation" stage, where a total of N_i interstitials are inserted one at a time at a constant rate r, followed by an "annealing" stage, where the system evolves without further disturbance. Throughout the simulation the system is subjected to zero external stress, and its temperature, defined in terms of the average total kinetic energy of all the particles, is maintained within certain limits about a mean value $T = 0.2$ by rescaling of the velocities. This temperature is about 30% of bulk melting.

We present data on three simulations which involve different combinations of r and N_i as shown in Table I. One can define an effective rate $R(t) = rf(t)$, where $f(t)$ is the fraction of interstitials in the system at time t. The average of $R(t)$ over the time interval of insertion, also given in Table I, provides a measure of the strength of the disturbance. It will be seen that amorphization is achieved under condition C but not under A or B.

Figure 1 shows the density response during insertion and relaxation. An initial density decrease indicates that the lattice overexpands to accommodate the additional particles; this effect, however, saturates after about fifty insertions. Once the insertion stops the system shows a tendency to densify, the extent of recovery depending on the extent of the perturbation. The potential-energy response, shown in Fig. 2, is consistent with the pattern of density behavior. As a manifestation of defect-

TABLE I. Insertion rate r and total number of interstitials introduced N_i for the three simulations. $\bar{R}$ is an effective rate.

	r	N_i	$\bar{R}$
A	5.95	160	0.702
B	14.71	80	0.936
C	14.71	160	1.736

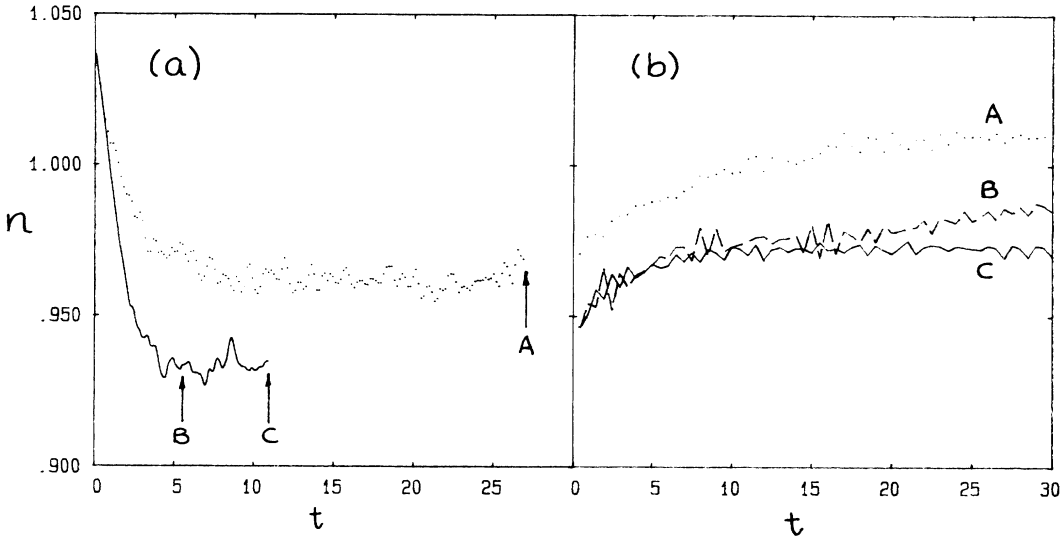

FIG. 1. System density (a) during interstitial insertion and (b) during relaxation. Arrows indicate times at which insertions are stopped.

concentration dependence, simulations B and C show different relaxations in density and potential energy even though the steady-state values show no changes with further insertion.

To follow the structural evolution we show in Fig. 3 the radial distribution function at the ends of the two stages. At the end of insertion, A and B still retain the structure of an fcc lattice although there is considerable broadening of the near-neighbor peaks, and during relaxation they clearly evolve toward a more crystalline structure. Particularly significant during the relaxation process is the growth of the second-neighbor peak for an fcc lattice at $r=1.56$. On the other hand, simulation C also retains some remnants of the fcc structure at the end of the insertion, but then it relaxes to a random close-packed structure which is identifiable by the absence of the second-neighbor peak of the fcc lattice and by the split second-neighbor peak in a liquid at the same density. On this basis we conclude that an amorphization threshold has been exceeded in simulation C.

It is of interest to compare the amorphized structure of simulation C with that of a supercooled liquid. To obtain the latter we heat up system C to $T=0.75$ (melting point of a Lennard-Jones solid is 0.70) at constant

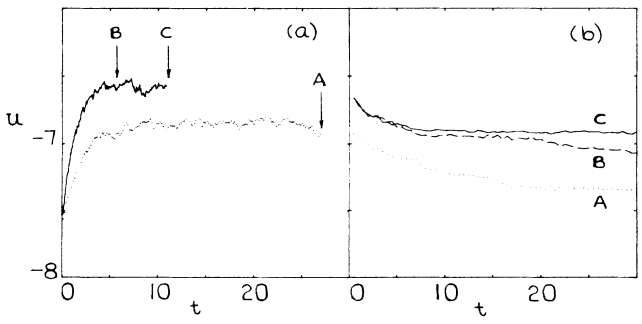

FIG. 2. Same as Fig. 1 except that response is the potential energy (per particle).

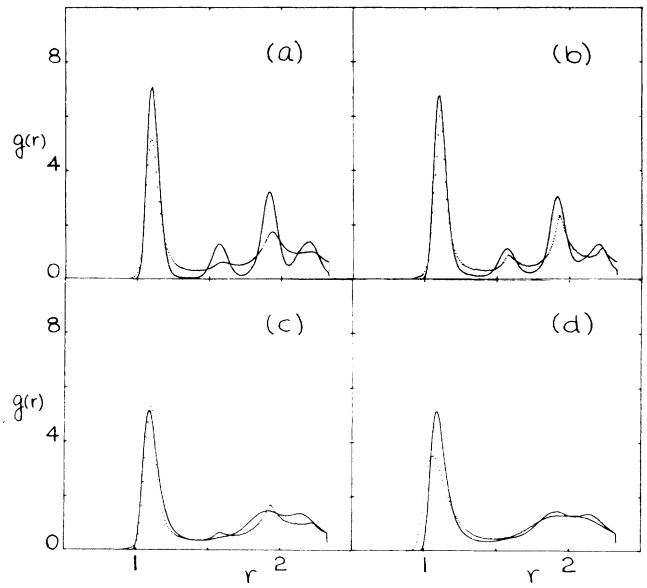

FIG. 3. Pair distribution function $g(r)$ after interstitial insertion (dotted curve) and after relaxation (solid curve) for simulations (a) A, (b) B, and (c) C. (d) Comparison of the amorphous structure from (c), which is indistinguishable from the $g(r)$ for a quenched liquid, with a liquid at $T=0.75$ (dotted curve).

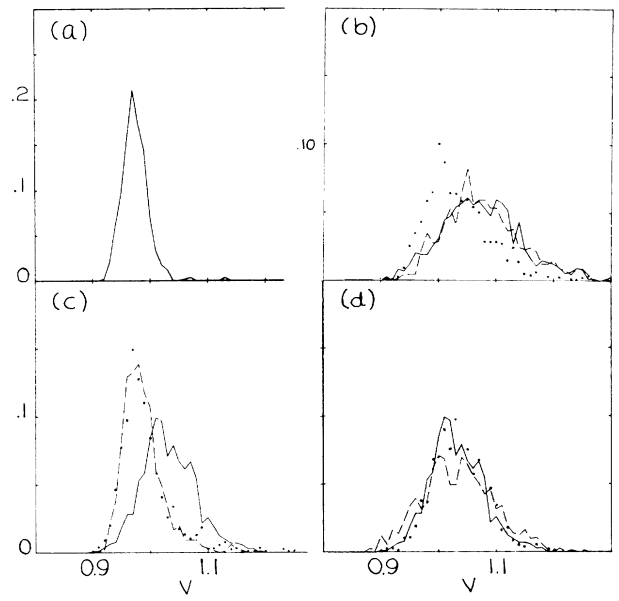

FIG. 4. Distribution of volume of Voroni polyhedra: (a) single crystal, (b) after interstitial insertion, (c) after relaxation for $t=30$; results for simulations A, B, and C are denoted by dotted, dashed, and solid curves, respectively. (d) Comparison of C with a quenched liquid at $T=0.2$ (dotted curve) and a liquid at $T=0.75$ (dashed curve).

volume, and after the liquid is well equilibrated the system is quenched to $T=0.2$ again at constant volume. We find the $g(r)$ of the resulting supercooled liquid to be indistinguishable from that of system C [Fig. 3(c)]. As a variation of our method of supercooling, we have also quenched to $T=0.001$ and heated up to 0.2, both at constant pressure. The two supercooled states at $T=0.2$, differing in density by 0.2% and in potential energy per particle by less than 1%, give the same $g(r)$.

The mean square displacements $\langle R^2(t)\rangle$ at the end of the irradiation stage in simulations A, B, and C are found to be proportional to the elapsed times, thus suggesting that atomic displacements are not much influenced by the interstitial insertion rate. Over the time interval of relaxation $\langle R^2(t)\rangle$ shows that there is still significant particle mobility in all three simulations; the process is most pronounced in B which most likely is associated with the formation of new (111) planes.[3]

To analyze the topological structure of the defective crystalline states A and B, and the amorphous state C, we have constructed the Voronoi polyhedra from these atomic configurations. Figure 4 shows the volume distribution of these polyhedra for the three simulations, along with those of reference systems, the single crystal, a liquid at the same density as C, and a quenched liquid at the same temperature and density as C. Notice that B and C are similar at the end of insertion [Fig. 4(b)], whereas after relaxation A and B resemble the single crystal while C is similar to the quenched liquid. We have also examined the distribution of number of faces n_f of the polyhedra. In all cases the component with the greatest weight is $n_f=14$, although in the amorphous state this component is less dominant, 0.39 for C as compared to 0.45 for A and B, and 0.42 for the single crystal. For the liquid at $T=0.75$ the relative weight of $n_f=14$ is 0.32. There is a tendency for the n_f distribution in the amorphous state to show a more pronounced tail at $n_f=16$ and 17.

TABLE II. Elastic constants averaged over three equivalent components and bulk modulus for the three simulations and reference systems of a single crystal and a quenched liquid, all at $T=0.2$. In the case of simulation C, the individual components are shown in parentheses to give an indication of directional equivalence.

System	C_{11}	C_{12}	C_{44}	B_t
Single crystal	533	146	136	275
A	469	175	111	273
B	424	180	105	261
C	(293,230,240)	(247,208,141)	(58,44,16)	217
	254	199	39	
Quenched liquid	264	219	39	234

Elastic constants of amorphized solids can be studied by Brillouin scattering, and it has been observed by charged-particle irradiation that a reduction of $\simeq 40\%$ in the elastic shear modulus can occur even before the amorphous state is reached.[5,6] We have calculated the adiabatic elastic constants of the three systems at the end of relaxation using the fluctuation formula derived recently.[7] The results are given in Table II along with the values obtained for the perfect crystal. One sees that in the defective crystals A and B there is a decrease in C_{11} and C_{44} while C_{12} increases somewhat. For the amorphous system C the effects are much more pronounced, and the values of C_{ij} are again close to those of the quenched liquid. The reduction of C_{11} and C_{44} in the amorphous state is primarily due to fluctuations in the stress tensor in the amorphous state; on the other hand, an increase in C_{12} is already evident in the contributions from static correlations (Born term), reflecting the onset of a more isotropic structure. If we assume that the bulk modulus B_t is given by $(C_{11}+2C_{12})/3$, there is essentially no change for A and B, whereas for C the decrease is significant, the magnitude of reduction being within the range of experimental observations.

In summary we have found that the defect-induced amorphization process is both rate and concentration dependent, and the resulting amorphized structure is similar to that of a quenched liquid. The combined re-

quirements of rapid insertion rate, $\simeq 10^{13}$ interstitials/s (in argon units), and an interstitial concentration level of about 25% are considerably beyond the conditions of current ion-beam irradiations. Thus there is no conflict between our findings and the fact that amorphization has not been achieved in pure metals. A similar study of binary component crystals is under way to investigate the role of compositional disorder and the effect of particle-size disparity in radiation-induced amorphization.

This work was supported by a grant from the National Science Foundation, No. CHE-8415078. We have benefitted greatly from our collaborations with the late Anees Rahman. One of us (S.Y.) would like to thank the Division of Materials Science, Argonne National Laboratory, for initial support and continued interest and the Institute of Theoretical Physics, University of California, Santa Barbara, for a stay during the manuscript writing stage. Computations reported here were carried out at the San Diego Supercomputer Center.

[1]D. F. Pedraza, J. Mater. Res. **1**, 425 (1986); Y. Limoge and A. Barbu, Phys. Rev. B **30**, 2212 (1984); *Phase Transformations during Irradiation,* edited by F. V. Nolfi (Applied Sciences, Englewood, NJ, 1983).

[2]See, for example, *Effects of Radiation on Materials: Twelfth International Symposium,* edited by F. A. Garner and J. S. Perrin (American Society for Testing Materials, Philadelphia, 1985), Special Technical Publication No. 870; *Ion Beam Modification of Materials,* edited by B. M. Ullrich (North-Holland, Amsterdam, 1985).

[3]First results of modeling radiation-induced amorphization by the introduction of Frenkel pairs or interstitials have been reported by Y. Limoge, A. Rahman, H. Hsieh, and S. Yip, J. Non-Cryst. Solids (to be published).

[4]M. Parrinello and A. Rahman, J. Appl. Phys. **52**, 7182 (1981).

[5]M. Grimsditch, Phys. Rev. Lett. **52**, 2379 (1984).

[6]M. Grimsditch, K. E. Gray, R. Bhadra, R. T. Kampwirth, L. E. Rehn, Phys. Rev. B **5**, 883 (1987).

[7]J. R. Ray, M. Moody, and A. Rahman, Phys. Rev. B **32**, 733 (1985).